Article

pubs.acs.org/Biomac

Polymeric Display of Proteins through High Affinity Leucine Zipper Peptide Adaptors

Patricio O. Craig, Vanina Alzogaray, and Fernando A. Goldbaum*

Fundación Instituto Leloir e Instituto de Investigaciones Bioquímicas de Buenos Aires, IIBBA-CONICET, Buenos Aires, C1405BWE, Argentina

Supporting Information

ABSTRACT: The polymeric display of proteins is a method that could be used to increase the immunogenicity of antigens and to enhance the interaction strength of binding domains for their target ligands through an avidity effect. However, the coupling of proteins to oligomeric scaffolds is challenging. The chemical conjugation and recombinant fusion techniques have limitations that prevent their general use. In this work we describe a simple and effective method for coupling proteins to the decameric structure of *Brucella abortus* Lumazine Synthase based on the use of a pair of high affinity heterodimeric coiled coil peptides complementary fused to the scaffold and the target protein. Results obtained with a series of proteins demonstrate the capability of this approach to generate polyvalent particles. Furthermore, we show that the method is able to increase the immunogenicity of antigens and produce polyfunctional particles with promising biomedical and nanotechnological applications.

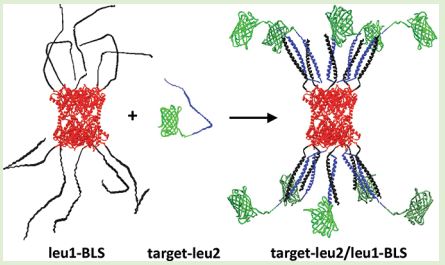

INTRODUCTION

The multiple display of molecules produced by the coupling to polymeric scaffolds has important applications. It could be used to increase the interaction strength of domains with their cognate ligands through an avidity effect[1−4] and to increase the immunogenicity of antigens for vaccine development.[5,6] There is a clear correlation between the structural repetitiveness and the immunogenicity of antigens.[7] The classical examples are the virus like particles (VLPs), which are highly immunogenic proteins composed of a repetitive array of subunits that are marginally immunogenic in the monomeric form.[8] The immunogenicity of polymeric particles is due, among other factors, to their ability to promote an efficient cross-linking of the B cell receptors.[9] This phenomenon produces the activation and proliferation of the B lymphocytes, the secretion of antibodies, and the induction of T lymphocyte response. The most successful examples of the use of VLPs for the development of protective immune responses in humans are the current vaccines against hepatitis B[10] and human papilloma virus.[11] This kind of particles have also been used as carriers to enhance the immunogenicity of molecules attached to their structure,[8,12] constituting an attractive approach for the development of immunological responses against a wide variety of microorganisms. However, the coupling of molecules to oligomeric scaffolds is challenging. The chemical conjugation and genetic fusion strategies[6,13] commonly used have several limitations. The delicate balance that exist between the conjugation yield, the conditions used for the coupling reaction, and the possible modification of multiple sites could affect the heterogeneity and stability of the products in the chemical conjugation procedures.[1,14−18] On the other hand, interactions between the subunits and target molecules usually prevent the proper folding and assembly of the polymeric particles in the recombinant fusion approach.[6] Although there are some successful examples of the polyvalent display of proteins through recombinant fusion to VLPs,[19−21] this strategy is limited by the size of the coupled ligand and is mostly used for the display of small peptides. These antigens, however, are usually poor immunogens to elicit protective antibody responses against pathogens due to their conformational flexibility and lack of a well-defined three-dimensional structure. To produce neutralizing antibodies, the immune system has to be exposed to whole proteins in their native conformation. Therefore, the development of strategies for the polymeric display of native proteins is valuable.

Noncovalent coupling methods have emerged as an alternative to chemical conjugation and recombinant fusion techniques. This modular approach is based on the specific interaction of molecular adaptors complementary fused to the structure of the coupling partners. A few methods have been proposed for the noncovalent coupling of proteins to VLPs,[22−24] but these usually involve the recombinant fusion of the target and/or the scaffold proteins to large protein adaptors. This feature would restrict the general applicability of these methods due to the potential interaction of the fused proteins during the folding stage. In principle, small adaptors like coiled coil peptides could be better tolerated. These peptides have been widely used as oligomerization modules and for the noncovalent coupling of simple molecules.[25] However, their use for the noncovalent coupling of ligands to polymeric

Received: December 31, 2011
Revised: February 24, 2012
Published: February 28, 2012

particles has been limited.[26−28] This is probably due to an increased tendency of the peptides to homodimerize through avidity interactions in the context of the repetitive scaffold and the subsequent cross-linking and aggregation of the particles. This phenomenon would be even more important when higher order oligomers are used.

Oligomeric scaffolds smaller than the VLPs may be advantageous for the polyvalent display of proteins. *Brucella* spp. lumazine synthase (BLS) is an enzyme that catalyzes an intermediate step in the biosynthesis of riboflavin in bacteria, fungi, and plants.[29,30] It has a decameric structure formed by 17 kDa subunits arranged as dimer of pentamers.[30−32] It is a powerful immunogen capable of eliciting strong humoral and cellular responses in animals inoculated either with the protein or with a plasmid coding to its sequence.[33,34] The immunogenicity of BLS is related to its oligomeric structure, its capacity to activate dendritic cells,[35] and its high thermodynamic stability and resistance to proteolysis,[30] which may increase its half-life inside organisms. In previous works we have successfully used BLS as a carrier to enhance the immunogenicity of short peptides fused to its structure.[36] We also demonstrated that it is possible to couple proteins of moderate size (9−18 kDa) to the structure of BLS by recombinant fusion.[37−39] This method allowed us to obtain well folded and stable decameric particles with enhanced immunogenicity and functional avidity compared to the isolated species. However, the constructs are expressed almost completely as inclusion bodies in *E. coli* and require refolding steps that have been proved to be unsuccessful in some cases.

In this work, we evaluate a novel modular coupling method based on the noncovalent interaction of a set of high affinity heterodimeric coiled coil peptides[40] complementary fused to the structure of BLS and the target protein. The fused peptides do not significantly interfere with the folding process of the scaffold and the target protein, and the coupling is simply produced by in vitro mixing the complementary species after their independent expression and purification.

To test the performance of this method we used a variety of proteins of unrelated functions and folds, and characterized the structure of the polymeric species obtained. The results presented here demonstrate that high affinity heterodimeric coiled coil peptides could be used for the noncovalent coupling of proteins to BLS, and highlight the use of this method for the production of polymeric particles for vaccine development and polyfunctional particles for nanobiotechnological applications.

MATERIALS AND METHODS

Assembly and Purification of Polyvalent Particles. The heterodimeric coiled coil peptides leu1 and leu2 were used to produce the noncovalent coupling of proteins to the structure of BLS. For this aim we used stock solutions of purified leu1-BLS (∼0.5 mg/mL) in 50 mM Tris/HCl, 8 M urea, 5 mM EDTA, 1 mM PMSF, pH 8.5, and purified leu2 or leu2 fusion proteins (∼0.5 mg/mL) in 50 mM Tris/HCl, 5 mM EDTA, 1 mM PMSF, 0.15 M NaCl, pH 8.5 (buffer A). Prior to the coupling process the proteins were incubated at 35 °C for 15 min to help the dissociation of possible homodimers of leu2 and leu1. After this, the coupling was produced by a rapid 1/10 dilution of the stock solution of leu1-BLS in a solution containing a 1.2 molar excess of leu2 or leu2 fusion proteins in buffer A, and incubation at room temperature for 15 min. Typically, 10 mL of solution containing the complex formed was concentrated to ∼0.5 mL by ultrafiltration using a centriprep Ultracel 10 K membrane device (Millipore, Billerica, MA, U.S.A.) and purified by size exclusion chromatography on a Superose 6 column (GE Healthcare Bio-Sciences AB, Uppsala, Sweden) using buffer A supplemented with 0.05% Tween 20. The complexes obtained were frozen using liquid nitrogen and stored at −80 °C. For the assembly and purification of the C-RBD3 complex we used buffer A containing 1 M NaCl concentration.

Circular Dichroism. The CD spectra of the proteins in the far UV region (250−200 nm) were measured on a JASCO J-810 spectropolarimeter at different experimental conditions (buffer composition, temperature, NaCl, and urea concentration), using quartz cuvettes of either a 1 or 5 mm path length. Samples were incubated at least 1 h before taking CD measurements. In general, the data was converted to molar ellipticity $[\theta]$ per dmol of protein (in units of deg cm^2 dmol$_{prot}^{-1}$). In the case of leu1-BLS, the CD spectra is shown in molar ellipticity $[\theta]$ per dmol of residues (in units of deg cm^2 dmol$_{res}^{-1}$) using a mean residue weight value of 111.3 g/mol. Unfolding of the proteins was monitored by the change in their molar ellipticity at 222 nm as a function of denaturant concentration. The CD spectra of RBD3 and VP8 was obtained from previous work,[37,38] and the one of eGFP was theoretically calculated with the k2d program[41] (http://www.embl.de/∼andrade/k2d/) using the reported structure of this protein (pdb code 1QYO).[42]

Light Scattering. The M_w and R_h of the protein samples was determined on a Precision Detectors PD2010 light scattering instrument tandemly connected to a high-performance liquid chromatography system, including a Waters 486 UV detector, and a LKB 2142 differential refractometer. The protein complexes were run on a Superose 6 column (GE Healthcare Bio-Sciences AB, Uppsala, Sweden). C-leu2, C-VP8, and C-eGFP were eluted in buffer A containing 0.05% Tween 20, whereas C-RBD3 was eluted in buffer A containing 0.05% Tween 20 and 1 M NaCl. Leu1-BLS was run on a Superdex 200 column (GE Healthcare Bio-Sciences AB, Uppsala, Sweden) and eluted with 50 mM Tris/HCl, 0.15 M NaCl, 5 mM EDTA, 1 mM PMSF, 8 M urea, and pH 8.5 buffer. All separations were performed at a 0.5 mL/min flow rate. The elution was monitored by measuring the static light scattering at 90° (SLS), the UV absorption at 280 nm (UV_{280}), and the refractive index (RI) signals. The data was recorded on a PC computer and analyzed with the Discovery32 software supplied by Precision Detectors. The molecular weight of each sample was calculated by the analysis of the SLS and RI signals, and comparison of the results with the ones obtained for BSA as a standard (M_w 66.5 kDa). This procedure, commonly known as the "two detector method",[43,44] is summarized in the Supporting Information. The R_h of the proteins was calculated from the analysis of the dynamic light scattering signal of the elution peak.

Thermal Denaturation. The heat-induced denaturation of BLS, leu1-BLS, and C-leu2 in 50 mM Tris/HCl, 0.1 M NaCl, pH 8 buffer in the presence or absence of urea was followed by measuring the CD signal at 222 nm of these proteins on a JASCO J-810 spectropolarimeter as a function of temperature. The samples were slowly heated by increasing the temperature with a Peltier system (Jasco). The temperature scanning was done on the 4−95 °C range at a speed of 4 °C/min. The molar ellipticity at 222 nm was measured every 0.5 °C. Fast or slow cooling back to 6 °C (from 95 to 6 °C at a speed of 1 °C/min) showed no recovery of the ellipticity, demonstrating the irreversibility of the thermal unfolding transitions of C-leu2 and leu1-BLS in agreement with the irreversibility of the thermal unfolding transition of BLS. Thus, the T_m of the thermal transitions of leu1-BLS, C-leu2, and BLS are reported as apparent T_m.

Immunization. Five female Balb/c mice were intraperitoneally immunized with 80 μg C-RBD3 in 50 mM Tris/HCl, 1.2 M NaCl, 0.8 M urea, pH 8 buffer, and boosted on day 14 with the same dose. As a control, five female Balb/c mice were intraperitoneally immunized with a mixture of 31 μg of RBD3-leu2 and 38 μg of BLS in 50 mM Tris/HCl, 1.2 M NaCl, 0.8 M urea, pH 8 buffer, and boosted on day 14 with the same dose. Sera were obtained at 21, 35, and 138 days after the first immunization. Experiments involving animals were approved by the Institutional Animal Care and Use Committee of the Fundación Instituto Leloir (IACUC-FIL) according to the Principles for Biomedical Research involving animals of the Council for International Organizations for Medical Sciences and provisions stated in the Guide for the Care and Use of Laboratory Animals.

ELISA Assays. Standard ELISA procedures were followed to measure antibody response against RBD3 and BLS. Nunc Maxisorp plates were coated with 50 μL of GST-RBD3 or BLS proteins (0.2 μg/well). The wells were then blocked with PBS containing 1% skim milk. The same solution was used for further dilutions of the primary and secondary antibodies. Plates were washed at each step with PBS. The reactivity of the sera was revealed by incubation with peroxidase-conjugated polyclonal antibodies against mice IgG (Sigma, St. Louis, MO). The reaction was developed by adding 50 μL of a solution containing 2 μg/μL orthophenylenediamine and 0.03% H_2O_2 in 0.1 M citrate phosphate buffer, and was stopped with 50 μL of 4 N H_2SO_4. The absorbance at 492 nm of the chromophoric product was measured in an ELISA reader (SLT Lab Instruments). ELISA titers were calculated as the last dilution with an absorbance three times higher than the background. The values reported correspond to averages for each group of animals. For this analysis, the absorbance corresponding to the replicates of each immunization group was averaged at each dilution and compared with the cut off established.

Molecular Modeling. The theoretical structure of the leu1 and leu2 heterodimeric coiled coil peptides was carried out by homology modeling with Swiss-Model (http://swissmodel.expasy.org/)[45,46] using the crystal structure of the C-terminal region of striated muscle alpha-tropomyosin as template (pdb code: 1KQL[47]). The theoretical structure of C-leu2 was modeled with the Swiss-PdbViewer program (http://spdbv.vital-it.ch/)[48] by fusing the C-terminal end of the leu1 peptide in the theoretical model of leu1/leu2 heterodimer to the structure of BLS (pdb code: 1DIO[49]) through a pentapeptide linker of sequence GSGSG. The theoretical structures of C-eGFP, C-VP8, and C-(VP8+eGFP) were generated with the Swiss-PdbViewer program by fusing the N-terminal end of leu2 in the theoretical model of C-leu2 to the C-terminal end of the structures of eGFP (pdb code: 2Y0G[50] and the model of the 62−224 region of the VP4 protein of BRV (VP8) through the pentapeptide linker GSGSG. The structure of VP8 was obtained by homology modeling with Swiss-Model using the crystallographic structure of $VP8_{62-224}$ of Rhesus rotavirus as template (pdb code: 1KQR[51]).

Fluorescence. The fluorescence of eGFP was measured on an LS 50B PerkinElmer luminescence spectrometer. A 4 nm bandwidth slits was used for excitation and emission. The excitation wavelength was set to 488 nm and the emission intensity was measured at 510 nm. All measurements were done at 25 °C in 50 mM Tris/HCl, 0.1 M NaCl, pH 8 buffer.

Binding of C-(eGFP+VP8) to Cells. HeLa cells were grown in standard conditions. Approximately 0.5×10^5 cells were transferred to cell culture plates containing microscope coverslips and incubated overnight at 37 °C in 10% CO_2. Then, the cells were washed with Hank's buffered salt solution (HBSS, Gibco, U.S.A.) and fixed using 4% paraformaldehyde for 15 min. The coverslip containing the cells was blocked with TBS buffer 1% BSA for 30 min, washed with TBS, and incubated with 5 μg of C-eGFP or an equimolar amount of C-(eGFP+VP8) in TBS buffer 1% BSA for 30 min at room temperature. Finally, the coverslips were mounted on microscope slides and analyzed in an LSM 510 confocal microscope (Carl Zeiss, Germany).

RESULTS AND DISCUSSION

Noncovalent Coupling through Heterodimeric Coiled Coil Peptides. In previous works, we used a recombinant fusion approach to couple proteins to the structure of BLS.[37−39] However, all the proteins tested were expressed as inclusion bodies in *E. coli* and required a refolding step that not always succeeded. Therefore, we decided to implement a noncovalent coupling strategy based on the use of high affinity heterodimeric peptides complementary fused to the structure of BLS and the target protein. This approach allows for the independent folding of the target protein and the scaffold, and the coupling could be simply produced by mixing the complementary species after their independent expression and purification. The rationale behind this method is that the fusion of the heterodimeric peptides to the structure of the scaffold and the target protein would be better tolerated than the direct fusion of both proteins.

To develop this method we used a set of high affinity heterodimeric coiled coil peptides described previously.[40] Specifically, we used the 43-mer peptides $RR_{12}EE_{345}L$ and $EE_{12}RR_{345}L$ that we will call for convenience leu1 and leu2, respectively. These peptides are derived from the structure of the leucine zipper VBP protein and have been engineered to destabilize homomeric interactions and favor the heterodimeric species. The isolated peptides have no structure at room temperature but when mixed they arrange as a heterodimeric coiled coil of high thermodynamic stability ($K_d = 1.3 \times 10^{-11}$ M).[40] It has to be noted, however, that although the isolated peptides are disordered they have some tendency to form homodimers at low temperatures. Therefore, we decided to fuse leu1 to the structure of BLS because this peptide has a lower tendency to dimerize than leu2.

The fusion of leu1 to the structure of BLS was carried out at the N-terminal end of the protein because it is a flexible region that does not contribute to the stabilization of the native structure and was previously shown to tolerate the insertion of peptides and small protein domains.[36−39] On the other hand, leu2 was fused to the C-terminal end of the target proteins (Figure 1). In both cases, the peptides were fused to the proteins through a flexible and hydrophilic pentapeptide linker (GSGSG) to minimize any possible interference with the proper folding of the proteins and to favor the mutual recognition of the heterodimeric peptides.

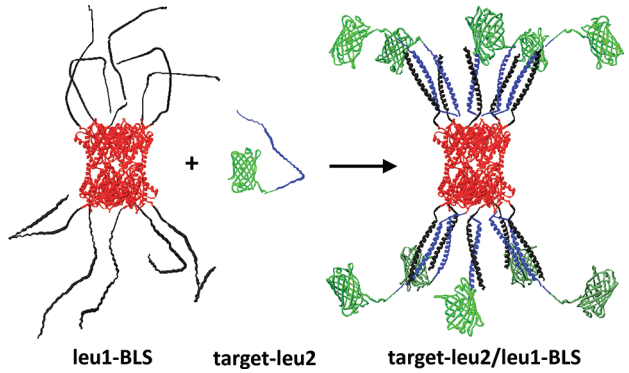

Figure 1. Noncovalent coupling of proteins to the structure of BLS. The leu1 and BLS modules in the structure of the leu1-BLS fusion protein are colored black and red, whereas the leu2 and target protein modules in the other fusion are colored blue and green, respectively.

Production and Characterization of leu1-BLS. The leu1-BLS fusion protein was cloned in the pET11a vector and expressed in *E. coli* at high levels, both at 28 and 37 °C. However, the protein was obtained as inclusion bodies and no soluble fraction was observed. The solubilization of the inclusion bodies in 8 M urea and dialysis against buffer produced the precipitation of the material again. To investigate the cause of this phenomenon, we purified the protein in denaturant conditions and characterized its conformational state at decreasing urea concentrations. The purification was carried out by anion exchange chromatography in the presence of 8 M urea. The purified protein was characterized by measurement of the molecular weight by size exclusion chromatography coupled to a static light scattering detector

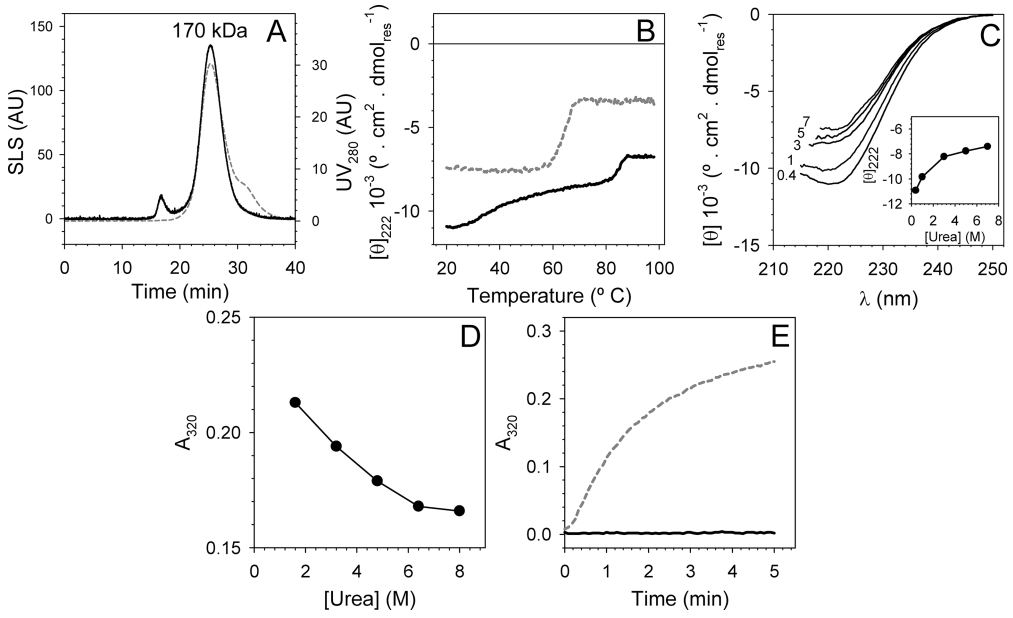

Figure 2. Structural analysis of leu1-BLS. (A) SEC-SLS analysis of leu1-BLS. The protein was loaded in a Superdex 200 HR 10/30 and eluted with buffer containing 8 M urea. The elution was monitored by measuring the light scattering at 90° (black continuous line) and UV absorption at 280 nm (gray dashed line) signals. (B) Thermal unfolding of leu1-BLS. The transition was followed by measuring the CD signal at 222 nm as a function of temperature in a buffer containing 7 (gray dashed line) and 0.4 M urea (black continuous line). (C) CD spectra of leu1-BLS at varying urea concentrations (0.4−7 M). The inset shows the signal at 222 nm of the protein as a function of urea. (D) Scattering signal of leu1-BLS as a function of urea concentration. The scattering was evaluated by measuring the UV absorbance of the protein sample at 320 nm. (E) Inhibition of leu1-BLS aggregation by addition of leu2. The time curse of leu1-BLS aggregation was evaluated by measuring the turbidity produced by a 1/10 dilution of a stock solution of leu1-BLS (in 8 M urea), with buffer (gray dashed line) or buffer containing a 2-fold molar excess of peptide leu2 (black continuous line). The turbidity was evaluated by the increase in the absorption of UV light at 320 nm as a function of time. All the experiments were done using a 50 mM Tris/HCl, 0.1 M NaCl, pH 8 buffer.

(SEC-SLS), and secondary structure content by circular dichroism (CD) spectroscopy.

The SEC-SLS analysis demonstrated that in 8 M urea leu1-BLS elutes as a complex broad peak with an average molecular weight of 170 kDa (Figure 2A) compatible with an average stoichiometry of 7.6 monomers per particle (M_w monomer: 22.2 kDa). This result was interpreted as the coelution of pentameric and decameric species of leu1-BLS in accordance with the oligomeric state of native BLS, which corresponds to a dimer of pentamers. The oligomeric state of the particles suggested that the BLS modules of the fusion protein were properly folded in the condition of the experiment, in agreement with the resistance of this protein to urea denaturation.[30] This conclusion was supported by the significant amount of secondary structure observed in the CD spectra of the protein (Figure 2C), and most importantly by the similarity between its thermal unfolding curve in 7 M urea (apparent Tm: 64 °C, Figure 2B) and that of BLS under the same conditions (66 °C).[37]

When the urea concentration was decreased below 6 M, we observed a significant increase in the CD signal of the protein and a progressive increase of turbidity in the sample (Figure 2C,D). These results were interpreted as a consequence of the homodimerization of leu1 in the decameric structure of the fusion protein and subsequent cross-linking and aggregation of the oligomeric particles. At 0.4 M urea, the protein that remained soluble presented a complex thermal unfolding behavior with two transitions (Figure 2B). The component of higher stability showed a cooperative transition with an apparent T_m of 85 °C compatible with the conformational stability of BLS under this condition,[37] whereas the component of lower stability showed a broad unfolding transition between 25 and 75 °C with an apparent T_m around 41 °C, which we attributed to the unfolding and dissociation of leu1 homodimers in the context of the BLS particles. It has to be noted that, although leu1 has a reported T_m that is lower than 6 °C,[40] it is possible that the polyvalency of leu1-BLS would increase the thermodynamic stability of the homomeric interactions of leu1 through an avidity effect. This hypothesis is supported by the inhibition of the aggregation of leu1-BLS produced by the leu2 peptide. Figure 2E shows the turbidity signal produced when a stock solution of leu1-BLS in 8 M urea was diluted in a buffer without urea both in the absence and in the presence of an excess of peptide leu2. In the absence of leu2 a big increase in the turbidity was observed due to the aggregation of the protein. This aggregation was irreversible as the addition of leu2 did not reduce the turbidity of the solution. In contrast, no turbidity was observed when leu1-BLS was diluted in the presence of leu2, demonstrating that the interaction of this peptide with leu1 prevents the aggregation phenomenon. This dilution procedure was then used to couple proteins to the structure of BLS.

Structural Characterization of the Complex between leu2 and leu1-BLS. To set up the conditions for the noncovalent coupling of proteins to BLS and to characterize the structure of the minimal complex common to all polymeric particles produced by this method, we analyzed the assembly of leu2 and leu1-BLS.

Prior to the coupling, the stock solutions of leu1-BLS and leu2 were preincubated for 15 min at 35 °C to ensure the unfolding of possible homodimeric species of the peptides. For the coupling, a stock solution of leu1-BLS (0.8 mg/mL in 50

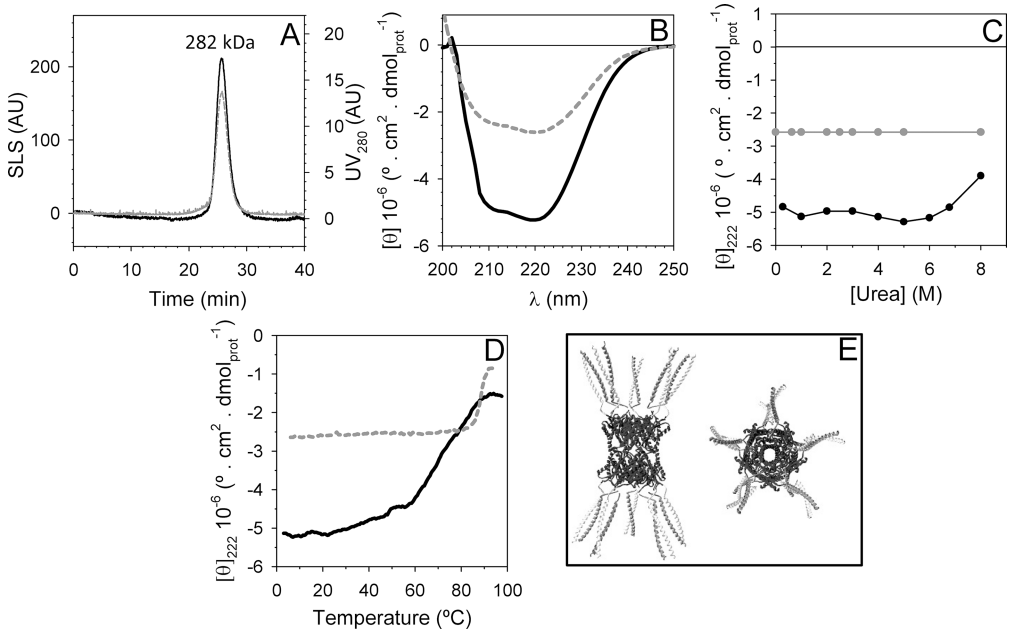

Figure 3. Structural characterization of C-leu2. (A) SEC-SLS analysis of C-leu2. The protein was loaded in a Superose 6 column. The chromatogram shows the light scattering at 90° (black continuous line) and the UV absorption at 280 nm (gray dashed line) signals of the eluate. The experimental M_w of the complex indicated in the plot was measured as described in Materials and Methods. (B) CD spectra of C-leu2 (black continuous line) compared to that of BLS (gray dashed line). (C) CD signal at 222 nm of C-leu2 (black line) and BLS (gray line) as a function of urea concentration. (D) Thermal unfolding curves of C-leu2 (black continuous line) and BLS (gray dashed line). The transitions were followed by measuring the CD signal at 222 nm as a function of temperature. (E) Theoretical model of C-leu2 (the BLS decamer is colored black, leu1 is colored light gray and leu2 is colored dark gray). All experiments were carried out in 50 mM Tris/HCl, 0.1 M NaCl, 5 mM EDTA, 1 mM PMSF, and pH 8 buffer.

mM Tris/HCl, 8 M urea, pH 8 buffer) was diluted 1/10 in a solution containing a 1.2-fold molar excess of leu2 in a 50 mM Tris/HCl, 5 mM EDTA, 1 mM PMSF, pH 8 buffer, and incubated for 15 min at room temperature. In these conditions, no increase in turbidity of leu1-BLS was observed, indicating the association of leu1 and leu2. After the coupling, the complex was purified by gel filtration to remove the excess of leu2 that remained unbound to leu1-BLS. The yield of the coupling reaction was estimated to be 60% relative to the original amount of leu1-BLS used, while the yield of the SEC purification step of the complexes was estimated to be around 65%. Although the coupling yield was good, we evaluated a variety of different conditions to test possible improvements. However, leu2/leu1-BLS molar ratios higher than 1.2, incubation times longer than 15 min or temperatures above room temperature did not increase the coupling yield and sometimes produced a slight decrease.

The structure of the complex between leu2 and leu1-BLS (C-leu2) thus obtained was analyzed by SEC-SLS and CD spectroscopy (Figure 3). The SEC-SLS analysis (Figure 3A) showed a monodisperse peak (polydispersity index M_w/M_n = 1.002) of 282 kDa, consistent with the complete coupling of leu2 (5.6 kDa) to the decameric structure of leu1-BLS (C-leu2 theoretical M_w: 279 kDa). The CD signal of the complex was higher than that of the isolated BLS protein due to the presence of the leu2/leu1 heterodimeric coiled coil structure (Figure 3B). In addition, urea and thermal unfolding experiments demonstrated a high thermodynamic stability of C-leu2 (Figure 3C,D). The urea unfolding analysis indicated the preservation of the structure of the complex up to 6 M urea concentration. The decrease observed in the CD signal above this concentration was attributed to the unfolding and dissociation of the heterodimeric coiled coil because BLS is resistant to this denaturant agent.[30] The signal of C-leu2 at 8 M urea approaches that of the isolated BLS module, suggesting a significant progression in the unfolding transition of the leu2 and leu1 modules of the complex under this condition. On the other hand, the thermal unfolding of C-leu2 evidenced a broad transition between 60 and 90 °C, with an apparent T_m of approximately 73 °C, in agreement with the value reported in the bibliography for the leu2/leu1 heterodimeric coiled coil.[40] In this regard, although the thermal stability of the isolated BLS module (apparent T_m 88 °C[30]) is higher than that of the heterodimeric pair of peptides, we did not observed a second component in the thermal denaturation curve of C-leu2 possibly due to an overlapping of both transitions or a concomitant aggregation of the protein upon unfolding of the coiled coil peptides in the absence of urea. In addition, we observed that the presence of high salt concentration (1.2 M NaCl) produced only a small decrease of 5 °C in the apparent T_m of the particles, and the recromatography of C-leu2 by gel filtration did not show any significant dissociation of the complex by dilution, providing further evidence of the thermodynamic and kinetic stability of the particles.

The results presented in this section indicate that the structures of BLS and the heterodimeric coiled coil peptides are preserved in the structure of the C-leu2 complex (Figure 3E).

Coupling of Proteins to the Structure of BLS through Coiled Coil Peptides. After establishing the assembly conditions and characterizing the structure of the C-leu2 complex, we tested the coupling of proteins to the structure of BLS. For this aim we used a set of five proteins of different size and function. This set included the dsRNA binding domain of murine Staufen protein (RBD3: 9 kDa), the variable region of a single domain llama antibody against the trans-sialidase enzyme of *Trypanosoma cruzi* (VHHtr: 13 kDa), the sialic acid binding

domain of bovine rotavirus capsid (VP8: 18 kDa), the ADP rybosyltransferase toxin from *Salmonella typhimurium* (SpvB: 25 kDa), and the enhanced green fluorescent protein from *Aequorea victoria* (eGFP: 26 kDa)

The proteins were cloned at the amino terminus end of the leu2 peptide in the pET11a vector using the GSGSG linker peptide to join both elements. The plasmids thus obtained encoding the RBD3-leu2 (14.4 kDa), VHHtr-leu2 (19.0 kDa), VP8-leu2 (24.6 kDa), SpvB-leu2 (30.6 kDa), and eGFP-leu2 (33.1 kDa) fusion proteins were transformed in *E. coli*. The expression assays demonstrated that all proteins were expressed in soluble form at 28 °C (Figure 4). Therefore they were purified from the cytoplasmic fraction of the bacteria, avoiding any refolding step. Initially we only purified the RBD3-leu2, VP8-leu2, and eGFP-leu2 fusion proteins. VHHtr-leu2 and SpvB-leu2 were not selected due to their low expression yield compared to the other proteins. The purifications were carried out by a combination of ion exchange chromatography and gel filtration. The SEC-SLS analysis demonstrated that VP8-leu2 and eGFP-leu2 are monomeric at low salt concentrations (M_w 27.8 and 39.8 kDa, respectively, at 50 mM Tris/HCl, 0.15 M NaCl, and pH 8). The analysis of RBD3-leu2 in the same conditions could not be measured due to the electrostatic interaction and adsorption of the protein to the column matrix. The adsorption was prevented by increasing the ionic strength of the buffer (50 mM Tris/HCl, 1.2 M NaCl, pH 8). In this condition all the leu2 fusion proteins eluted as dimers (M_w 25.3, 45.3, and 66.1 kDa for RBD3-leu2, VP8-leu2, and eGFP-leu2, respectively). This phenomenon was attributed to the homodimerization of leu2 promoted by the screening of repulsive electrostatic interactions at high salt concentration (leu2 pI ~ 11.0). This hypothesis was confirmed by the M_w of leu2 measured at low and high salt concentration (M_w 5.8 and 10.2 kDa, respectively).

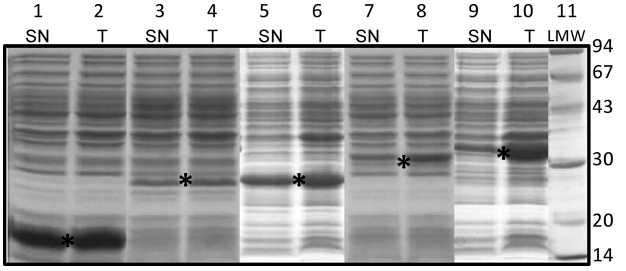

Figure 4. SDS-PAGE analysis of proteins fused to the leu2 peptide and expressed in *E. coli*. The soluble (SN) and total (T) fractions of the cells expressing RBD3-leu2 (lanes 1 and 2), VHHtr-leu2 (lanes 3 and 4), VP8-leu2 (lanes 5 and 6), SpvB-leu2 (lanes 7 and 8), and eGFP-leu2 (lanes 9 and 10) were analyzed. The M_w in kDa of the low molecular weight markers (lane 11) is shown on the right side of the figure. The bands corresponding to each protein are labeled with an asterisk.

After the purification, the proteins were coupled to the structure of leu1-BLS following the same procedure as described before for the C-leu2 complex. By this method we obtained the RBD3-leu2/leu1-BLS (C-RBD3), VP8-leu2/leu1-BLS (C-VP8), and eGFP-leu2/leu1-BLS (C-eGFP) complexes. The purification of these products was done by gel filtration. The yields of the coupling (~60%) and purification (~65%) steps measured for all proteins were similar to the ones

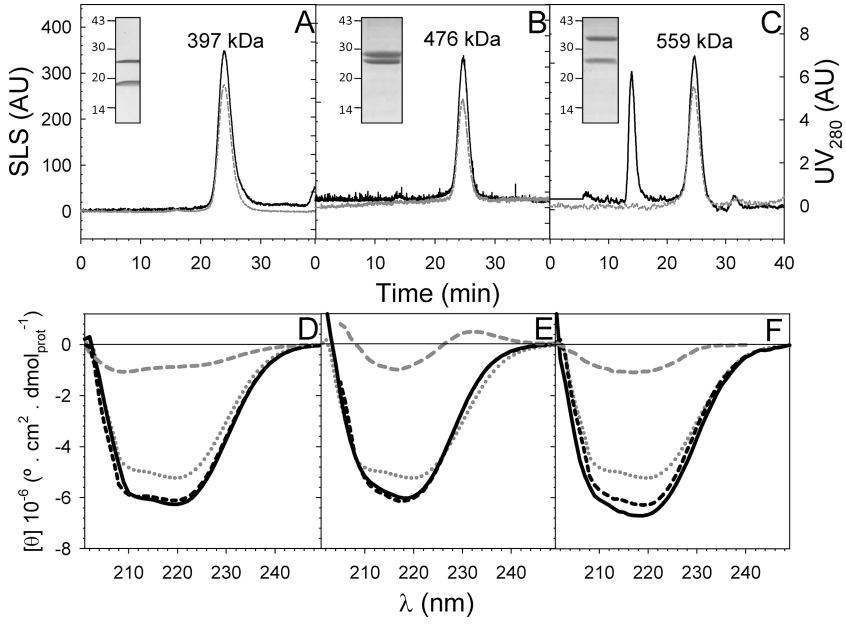

Figure 5. Structural characterization of the complexes formed between leu1-BLS and proteins fused to the leu2 peptide. (A-C) SEC-SLS analysis of the C-RBD3, C-VP8, and C-eGFP complexes, respectively. The proteins were loaded in a Superose 6 column. The chromatograms show the light scattering at 90 degree (black continuous line) and the UV absorption at 280 nm (gray dashed line) signals of the eluate. The experimental molecular weights of the different complexes were measured as described in Materials and Methods, and the values are indicated in each plot. The insets in A–C show the SDS-PAGE analysis of the peak observed in the chromatogram of each protein complex. The SLS peak observed ~14 min in (C) corresponds to traces of particulate material eluting at the void. (D-F) CD spectra of C-RBD3, C-VP8, C-eGFP and their corresponding modules, respectively. In each plot, the experimentally determined spectra of the complex (black continuous line) is compared to the theoretical spectra (black dashed line) calculated by the sum of the spectra of the corresponding target protein (RBD3, VP8, and eGFP, gray dashed line) and the C-leu2 complex (gray dotted line). All experiments were carried out in 50 mM Tris/HCl, 0.1 M NaCl, 5 mM EDTA, 1 mM PMSF, and pH 8 buffer. In the case of C-RBD3, the buffer contained additionally 1.2 M NaCl.

dx.doi.org/10.1021/bm201875p | *Biomacromolecules* 2012, 13, 1112–1121

obtained for the C-leu2 complex. The presence of 1.2 M NaCl in the assembly buffer of C-RBD3 did not produce any decrease in the coupling yield in spite of the favorable dimerization of the leu2 peptide in this condition. This is probably due to a fast equilibrium between the dimeric and monomeric species of leu2 under this condition, and the efficient competition of leu1 for binding to leu2. At the same time, the presence of 0.8 M urea in the assembly buffer would favorably shift the equilibria between monomeric and dimeric species of leu2.

The conformational state of the purified complexes was analyzed by different biophysical techniques. The SEC-SLS analysis (Figure 5A–C) indicated that all complexes eluted as single homogeneous peaks (polydispersity index $M_w/M_n \sim 1.001$) of a molecular weight (M_w: 397, 476, and 559 kDa for C-RBD3, C-VP8, and C-eGFP, respectively) compatible with the complete coupling of the proteins to the decameric structure of leu1-BLS (theoretical M_w: 367, 469, and 554 kDa for the C-RBD3, C-VP8, and C-eGFP decameric complexes, respectively). The elution peaks observed by gel filtration were analyzed by SDS PAGE and showed the presence of equimolar amounts of two bands corresponding to leu1-BLS and the respective target protein fused to the leu2 peptide. The hydrodynamic radius (Rh) of the particles obtained was ~7.5 nm as measured by dynamic light scattering (DLS). The CD spectra of the complexes (Figure 5D–F) was equivalent to the sum of the spectra of the isolated target protein and the C-leu2 complex (which includes the BLS, leu2, and leu1 modules), indicating the conservation of the secondary structure of the different modules in the structure of the complex.

Furthermore, thermal unfolding experiments indicated that the C-RBD3 and C-VP8 complexes are stable up to 50 and 60 °C, respectively, in agreement with the stability of the isolated RBD3 and VP8 proteins which are the modules of lower stability in the complexes. In addition, the fluorescence of C-eGFP was analyzed and revealed an excitation and emission spectra characteristic of the native eGFP protein. All these data indicate that the different modules are properly folded in the structure of the polyvalent particles.

To evaluate the kinetic stability of the complexes we incubated the C-VP8 complex with a 2.5 fold molar excess of eGFP-leu2. In this condition, it would be expected that at equilibrium 72% of the original VP8-leu2 associated with leu1-BLS would be displaced from the complex by competition with the excess of eGFP-leu2. However, after 16 h of incubation at 4 °C and analysis of the mixture by size exclusion chromatography, no significant amount of eGFP fluorescence was observed associated to the elution peak of the C-VP8 complex (see Figure S1 in the Supporting Information). This result demonstrates that no significant displacement of VP8-leu2 from the C-VP8 complex is produced by eGFP-leu2 under the conditions tested, indicating that the heterodimeric structure of the leu2 and leu1 peptides is very stable and has a very low dissociation rate constant.

Finally, it has to be noted that the complexes could be stored for weeks at 4 °C without any significant loss of material. Only an unspecific adsorption phenomenon to glass or plastic material was observed, but could be completely prevented by the addition of 0.05% Tween20 to the sample. For long-term storage the complexes were frozen at −80 °C in the presence of 0.05% Tween20 or 1% BSA, and resisted freeze thaw cycles without any significant loss of material.

Polyvalent Display of Proteins by Noncovalent Coupling to the Structure of BLS Increase the Immunogenicity of Antigens. To test the increase in the immunogenicity of antigens produced by the noncovalent coupling to the decameric structure of BLS, we used the RBD3 antigen, as we did before for the recombinant fusion strategy.[37] For this aim we used two experimental groups of mice. The first group was intraperitoneally inoculated with the C-RBD3 complex, whereas the second group was inoculated with an equimolar mixture of the isolated RBD3-leu2 and BLS proteins as control. The immunizations were carried out in the absence of adjuvants. Both groups were boosted with the same dose two weeks later and bled at days 21, 35, and 138 to evaluate the titer of anti-RBD3 and anti-BLS antibodies in the sera.

The control group produced no significant response toward the RBD3 antigen (titer <100), whereas the group inoculated with the C-RBD3 complex showed a high and persistent response toward this antigen (Figure 6), with titers of 3200 at

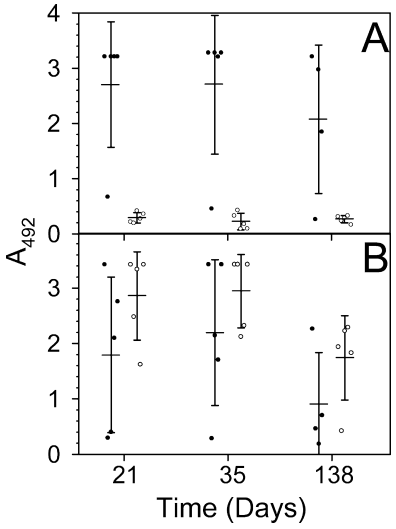

Figure 6. Time evolution of the anti-RBD3 (A) and anti-BLS (B) antibodies in the sera of mice inoculated with the C-RBD3 complex (black dots) or an equimolar mixture of RBD3-leu2 and BLS (white dots). The antibody response was evaluated by the absorbance at 492 nm produced in ELISA assays using a 1/100 dilution of the sera. The horizontal lines show the average signal of each group. The error bars correspond to the standard deviation of the replicates. One mouse of the test group died between days 35 and 138.

day 35 and 1600 at day 138. The increase in the immunogenicity of RBD3 was similar to that obtained using the recombinant fusion strategy,[37] suggesting no significant dissociation of the protein complex upon dilution in the inoculated animal. Indeed, only trace amounts of the protein complex (~0.1%) would be expected to dissociate upon dilution in the mice fluids based on the high affinity interaction between leu1 and leu2 (K_D 1.3×10^{-11} M) and the dose used in the experiment. These results demonstrate that the polyvalent display by noncovalent coupling to BLS is an effective method to increase the immunogenicity of antigens. This effect is even more important taking into account that RBD3 is an autologous antigen. Thus, the polyvalent display could overcome the tolerance of the mice to this self-antigen. The increase in immunogenicity was produced only when the antigen was coupled to the structure of BLS as the coadministration of RBD3-leu2 and BLS produced no

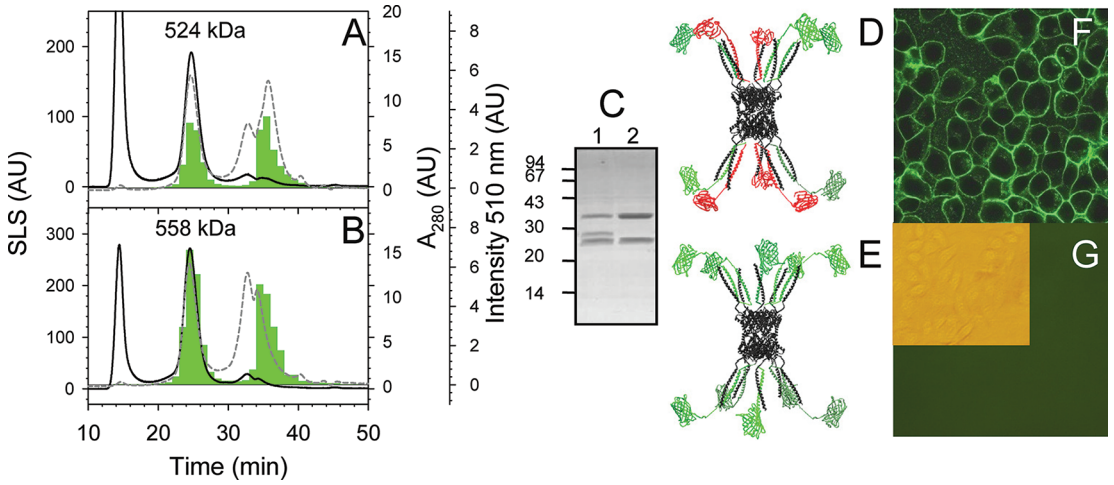

Figure 7. Bifunctional particle C-(VP8+eGFP) produced by the simultaneous coupling of VP8-leu2 and eGFP-leu2 to the structure of leu1-BLS. The figure shows the SEC-SLS purification and analysis of C-(VP8+eGFP) and C-eGFP particles (A and B, respectively). The elution was monitored by measuring the light scattering at 90 degree (black continuous line), the UV absorption at 280 nm (gray dashed line), and the eGFP fluorescence at 510 nm measured on fractions collected at 1 min time intervals (green bars). The M_w measured by SLS of the peaks corresponding to the elution of the protein complexes (~25 min) are indicated in each plot. The SLS peaks observed at the void (~15 min) corresponds to small amounts of particulate material. The peaks observed between 30 and 40 min correspond to the excess e-GFP-leu2, VP8-leu2 and leu1-BLS that remained uncoupled. (C) SDS-PAGE analysis of the elution peaks of C-(VP8+eGFP) (lane 1) and C-eGFP (lane 2). (D and E) Theoretical models of the C-(VP8+eGFP) and C-eGFP complexes, respectively. (F and G) Fluorescence microscopy images of HeLa cells incubated with the C-(VP8+eGFP) and C-eGFP complexes, respectively. Due to the absence of any signal in the fluorescence microscopy image of C-eGFP, a bright field image is also shown in the inset to demonstrate the presence of cells in the field.

significant response. This lack of response in the control sample also indicates that the fusion to the leu2 peptide by its own do not increase the immunogenicity of the antigen.

Finally, we observed high and persistent titers of anti-BLS antibodies in both experimental groups with titers as high as 12800 at day 35, and 1600 at day 138 for the control sample, and 3200 at day 35, and 800 at day 138 for the C-RBD3 sample. The slight decrease observed in the anti-BLS titer of the C-RBD3 sample compared to the control sample could be related to a lower accessibility of BLS in the structure of the complex.

Colocalization and Production of Polyfunctional Particles. The coupling through heterodimeric peptides represents a straightforward procedure to colocalize different proteins in the same polymeric particle. In this case, multifunctional particles could be produced simply by mixing leu1-BLS with different proteins attached to the leu2 peptide. This application was explored by the production of a bifunctional particle containing the VP8 and eGFP proteins. As mentioned before VP8 is a protein domain of bovine rotavirus capsid that binds to sialic acid found in the surface of cells, while eGFP is the green fluorescent protein from *Aequorea victoria*. The mixture of leu1-BLS with equimolar amounts of VP8-leu2 and eGFP-leu2 produced mixed polymeric particles C-(VP8+eGFP) with an average molecular weight of 524 kDa measured by SEC-SLS analysis (Figure 7). This value is intermediate to the theoretical molecular weight of the homogeneus C-VP8 (469 kDa) and C-eGFP (554 kDa) complexes. The elution peak of C-(VP8+eGFP) contained three components (leu1-BLS, VP8-leu2 and eGFP-leu2) as shown by SDS-PAGE analysis, and an amount of fluorescence relative to protein concentration 2-fold lower than that observed for C-eGFP as expected for the bifunctional particle.

The incubation of C-(VP8+eGFP) with HeLa cells produced a fluorescent label on the surface of the cells, demonstrating the colocalization of eGFP and VP8 in the same oligomeric particle. As a control, we also incubated the C-eGFP complex with HeLa cells. In this case no fluorescence was observed, discarding any nonspecific binding of the particle to the cells.

■ CONCLUSIONS

In this work we introduced a method for the polyvalent display of proteins based on the noncovalent coupling to the oligomeric structure of BLS. For this aim we used a pair of high affinity heterodimeric coiled coil peptides[40] complementary fused to the structure of BLS and the target protein. This method prevents any possible interaction between the scaffold and the target protein during the folding process due to their independent expression and purification. Then, the coupling is produced through the mixture of the complementary species.

In the current work we detected a tendency of leu1-BLS to self-associate through homomeric interactions of the leu1 peptide. These interactions were disrupted upon solubilization of the inclusion bodies in urea, and were totally blocked after coupling of the protein to the leu2 partner. On the other hand, all the proteins fused to the leu2 peptide were soluble expressed in *E. coli* avoiding any particular treatment of the samples. In principle, depending on any particular need, the target protein fused to the leu2 peptide could be expressed in different cell types for example to produce a specific post-translational modification or assistance of chaperones in the folding process.

Using this noncovalent strategy, we produced the complete coupling of a series of proteins to the structure of BLS, obtaining monodisperse decameric particles with all the protein modules properly folded. The high yield of the coupling procedure allowed an efficient usage of the recombinant proteins compared to chemical conjugation procedures that require a large excess of substrates due to low conjugation efficiencies. The high thermodynamic and kinetic stability of BLS and the heterodimeric coiled coil peptides used was manifested in the stability of the polyvalent particles obtained.

dx.doi.org/10.1021/bm201875p | *Biomacromolecules* 2012, 13, 1112–1121

In this work, we also demonstrated that the coupling of proteins to the structure of BLS could be used to increase the immunogenicity of antigens. The polyvalent display of RBD3 by noncovalent coupling to the structure of BLS was able to overcome the tolerance of mice to this self-antigen and produced an increase in the immunogenicity of RBD3 similar to that obtained with the recombinant fusion strategy.[37]

In addition, we showed that the coupling of proteins to BLS through heterodimeric peptides is an easy and straightforward procedure for preparing multifunctional particles. This scaffold could potentially colocalize up to 10 different protein or nonprotein functionalities, allowing the combination of a variety of functions like cell targeting, cell internalization, subcellular localization signals, fluorescent or radioactive tags, cytotoxic enzymes or other biological effectors in the same particle. Due to the multivalent nature of the display, the previous functions may also be combined with an increase in the interaction strength of binding domains for their target ligands through an avidity effect, or a high density of fluorescent proteins for increasing the brilliance of the particles and facilitate their tracking in single molecule experiments.

In the area of vaccine development the polyfunctional particles could be used to colocalize different antigens in the same particle. However, it is not clear whether this type of immunogen would have any advantage over the coadministration of multiple monospecific particles. In addition, the colocalization of antigens with coestimulatory molecules in the structure of BLS could probably be used to further increase the immunogenicity of the antigen or to switch the type of immunogenic response.

Due to the stochastic nature of the assembly process, the composition of the polyfunctional particles would be heterogeneous. The percentage of particles that colocalize a given set of elements would be inversely related to the number of elements used. This feature would determine the coexistence of particles with full colocalization and particles with partial or no colocalization. The presence of particles with partial colocalization could be a problem or not for some applications. However, if a sample with full colocalization is needed it might be possible to use different purification tags (HIS, FLAG, HA, MYC, etc.) for each type of protein and perform a multi tag purification of the assembly products.

The results presented in this work indicate that the noncovalent coupling of proteins to the structure of BLS through heterodimeric coiled coil peptides is a very useful method for vaccine development and also for the production of polyfunctional particles. This type of particles has also a great potential for molecular, cell biology, and nanobiotechnological applications.

■ ASSOCIATED CONTENT

Supporting Information

Description of protein and peptide production and purification, a summary of the "two detector" method used for the analysis of the M_w of proteins by SEC-SLS, and a study of the kinetic stability of the C-VP8 complex (Figure S1). This material is available free of charge via the Internet at http://pubs.acs.org.

■ AUTHOR INFORMATION

Corresponding Author

*Tel.: 54 11 5238-7500. Fax: 54 11 5238-7501. E-mail: fgoldbaum@leloir.org.ar.

Notes

The authors declare no competing financial interest.

■ ACKNOWLEDGMENTS

Thanks to Dr. Prat Gay and his lab for assistance with the CD spectroscopy measurements, Mariela Urrutia and Cecilia D'Alessio for providing the source material of two proteins studied, Paula Berguer for help in the ELISA assays, Gaston Mayol for his assistance in liquid chromatography separations, and Maria Jimena Ortega and Marta Bravo for DNA sequencing and confocal miscrocopy assistance.

■ ABBREVIATIONS

VLPs, virus-like particle; BLS, *Brucella abortus* Lumazine Synthase; SEC-SLS, size exclusion chromatography coupled to static light scattering detector; CD, circular dichroism; RBD3, dsRNA binding domain of murine Staufen protein; VHHtr, variable region of a single domain llama antibody against the trans-sialidase enzyme of *Trypanosoma cruzi*; VP8, sialic acid binding domain of bovine rotavirus capsid; SpvB, ADP rybosyltransferase toxin from *Salmonella typhimurium*; eGFP, enhanced green fluorescent protein from *Aequorea victoria*; C-leu2, leu2/leu1-BLS complex; C-RBD3, RBD3-leu2/leu1-BLS complex; C-VP8, VP8-leu2/leu1-BLS complex; C-eGFP, eGFP-leu2/leu1-BLS complex; R_h, hydrodynamic radius; DLS, dynamic light scattering.

■ REFERENCES

(1) Banerjee, D.; Liu, A. P.; Voss, N. R.; Schmid, S. L.; Finn, M. G. *ChemBioChem* **2010**, *11*, 1273−9.
(2) Gestwicki, J. E.; Cairo, C. W.; Strong, L. E.; Oetjen, K. A.; Kiessling, L. L. *J. Am. Chem. Soc.* **2002**, *124*, 14922−33.
(3) Zhang, J.; Tanha, J.; Hirama, T.; Khieu, N. H.; To, R.; Tong-Sevinc, H.; Stone, E.; Brisson, J. R.; MacKenzie, C. R. *J. Mol. Biol.* **2004**, *335*, 49−56.
(4) Pluckthun, A.; Pack, P. *Immunotechnology* **1997**, *3*, 83−105.
(5) Ludwig, C.; Wagner, R. *Curr. Opin. Biotechnol.* **2007**, *18*, 537−45.
(6) Jennings, G. T.; Bachmann, M. F. *Biol. Chem.* **2008**, *389*, 521−36.
(7) Bachmann, M. F.; Kopf, M. *Curr. Opin. Immunol.* **1999**, *11*, 332−9.
(8) Nieba, L.; Bachmann, M. F. *Mod. Aspects Immunobiol.* **2000**, *1*, 36−39.
(9) Bachmann, M. F.; Zinkernagel, R. M. *Immunol. Today* **1996**, *17*, 553−8.
(10) Raz, R.; Dagan, R.; Gallil, A.; Brill, G.; Kassis, I.; Koren, R. *Vaccine* **1996**, *14*, 207−11.
(11) Schiller, J. T.; Lowy, D. R. *Annu. Rev. Microbiol.* **2010**, *64*, 23−41.
(12) Tissot, A. C.; Renhofa, R.; Schmitz, N.; Cielens, I.; Meijerink, E.; Ose, V.; Jennings, G. T.; Saudan, P.; Pumpens, P.; Bachmann, M. F. *PLoS One* **2010**, *5*, e9809.
(13) Strable, E.; Finn, M. G. *Curr. Top. Microbiol. Immunol.* **2009**, *327*, 1−21.
(14) Patel, K. G.; Swartz, J. R. *Bioconjugate Chem.* **2011**, *22*, 376−87.
(15) Sen Gupta, S.; Kuzelka, J.; Singh, P.; Lewis, W. G.; Manchester, M.; Finn, M. G. *Bioconjugate Chem.* **2005**, *16*, 1572−9.
(16) Jegerlehner, A.; Tissot, A.; Lechner, F.; Sebbel, P.; Erdmann, I.; Kundig, T.; Bachi, T.; Storni, T.; Jennings, G.; Pumpens, P.; Renner, W. A.; Bachmann, M. F. *Vaccine* **2002**, *20*, 3104−12.
(17) Lechner, F.; Jegerlehner, A.; Tissot, A. C.; Maurer, P.; Sebbel, P.; Renner, W. A.; Jennings, G. T.; Bachmann, M. F. *Intervirology* **2002**, *45*, 212−7.
(18) Chatterji, A.; Ochoa, W.; Shamieh, L.; Salakian, S. P.; Wong, S. M.; Clinton, G.; Ghosh, P.; Lin, T.; Johnson, J. E. *Bioconjugate Chem.* **2004**, *15*, 807−13.

(19) Kratz, P. A.; Bottcher, B.; Nassal, M. *Proc. Natl. Acad. Sci. U.S.A.* **1999**, *96*, 1915−20.
(20) Vogel, M.; Vorreiter, J.; Nassal, M. *Proteins* **2005**, *58*, 478−88.
(21) Domingo, G. J.; Orru, S.; Perham, R. N. *J. Mol. Biol.* **2001**, *305*, 259−67.
(22) Chackerian, B.; Lowy, D. R.; Schiller, J. T. *J. Clin. Invest.* **2001**, *108*, 415−23.
(23) Gleiter, S.; Lilie, H. *Protein Sci.* **2001**, *10*, 434−44.
(24) Venter, P. A.; Dirksen, A.; Thomas, D.; Manchester, M.; Dawson, P. E.; Schneemann, A. *Biomacromolecules* **2011**, *12*, 2293−301.
(25) Apostolovic, B.; Danial, M.; Klok, H. A. *Chem. Soc. Rev.* **2010**, *39*, 3541−75.
(26) Wu, K.; Liu, J.; Johnson, R. N.; Yang, J.; Kopecek, J. *Angew. Chem., Int. Ed.* **2010**, *49*, 1451−5.
(27) Minten, I. J.; Hendriks, L. J.; Nolte, R. J.; Cornelissen, J. J. *J. Am. Chem. Soc.* **2009**, *131*, 17771−3.
(28) Wang, K. C.; Wang, X.; Zhong, P.; Luo, P. P. *J. Mol. Biol.* **2010**, *395*, 1088−101.
(29) Bonomi, H. R.; Marchesini, M. I.; Klinke, S.; Ugalde, J. E.; Zylberman, V.; Ugalde, R. A.; Comerci, D. J.; Goldbaum, F. A. *PLoS One* **2010**, *5*, e9435.
(30) Zylberman, V.; Craig, P. O.; Klinke, S.; Braden, B. C.; Cauerhff, A.; Goldbaum, F. A. *J. Biol. Chem.* **2004**, *279*, 8093−101.
(31) Klinke, S.; Zylberman, V.; Vega, D. R.; Guimaraes, B. G.; Braden, B. C.; Goldbaum, F. A. *J. Mol. Biol.* **2005**, *353*, 124−37.
(32) Klinke, S.; Zylberman, V.; Bonomi, H. R.; Haase, I.; Guimaraes, B. G.; Braden, B. C.; Bacher, A.; Fischer, M.; Goldbaum, F. A. *J. Mol. Biol.* **2007**, *373*, 664−80.
(33) Cassataro, J.; Pasquevich, K. A.; Estein, S. M.; Laplagne, D. A.; Velikovsky, C. A.; de la Barrera, S.; Bowden, R.; Fossati, C. A.; Giambartolomei, G. H.; Goldbaum, F. A. *Vaccine* **2007**, *25*, 4437−46.
(34) Cassataro, J.; Pasquevich, K. A.; Estein, S. M.; Laplagne, D. A.; Zwerdling, A.; de la Barrera, S.; Bowden, R.; Fossati, C. A.; Giambartolomei, G. H.; Goldbaum, F. A. *Vaccine* **2007**, *25*, 5958−67.
(35) Berguer, P. M.; Mundinano, J.; Piazzon, I.; Goldbaum, F. A. *J. Immunol.* **2006**, *176*, 2366−72.
(36) Laplagne, D. A.; Zylberman, V.; Ainciart, N.; Steward, M. W.; Sciutto, E.; Fossati, C. A.; Goldbaum, F. A. *Proteins* **2004**, *57*, 820−8.
(37) Craig, P. O.; Berguer, P. M.; Ainciart, N.; Zylberman, V.; Thomas, M. G.; Martinez Tosar, L. J.; Bulloj, A.; Boccaccio, G. L.; Goldbaum, F. A. *Proteins* **2005**, *61*, 1089−100.
(38) Bellido, D.; Craig, P. O.; Mozgovoj, M. V.; Gonzalez, D. D.; Wigdorovitz, A.; Goldbaum, F. A.; Dus Santos, M. J. *Vaccine* **2009**, *27*, 136−45.
(39) Ratier, L.; Urrutia, M.; Paris, G.; Zarebski, L.; Frasch, A. C.; Goldbaum, F. A. *PLoS One* **2008**, *3*, e3524.
(40) Moll, J. R.; Ruvinov, S. B.; Pastan, I.; Vinson, C. *Protein Sci.* **2001**, *10*, 649−55.
(41) Andrade, M. A.; Chacon, P.; Merelo, J. J.; Moran, F. *Protein Eng.* **1993**, *6*, 383−90.
(42) Barondeau, D. P.; Putnam, C. D.; Kassmann, C. J.; Tainer, J. A.; Getzoff, E. D. *Proc. Natl. Acad. Sci. U.S.A.* **2003**, *100*, 12111−6.
(43) Takagi, T. *J. Chromatogr.* **1990**, *506*, 409−416.
(44) Wen, J.; Arakawa, T.; Philo, J. S. *Anal. Biochem.* **1996**, *240*, 155−66.
(45) Arnold, K.; Bordoli, L.; Kopp, J.; Schwede, T. *Bioinformatics* **2006**, *22*, 195−201.
(46) Kiefer, F.; Arnold, K.; Kunzli, M.; Bordoli, L.; Schwede, T. *Nucleic Acids Res.* **2009**, *37*, D387−92.
(47) Li, Y.; Mui, S.; Brown, J. H.; Strand, J.; Reshetnikova, L.; Tobacman, L. S.; Cohen, C. *Proc. Natl. Acad. Sci. U.S.A.* **2002**, *99*, 7378−83.
(48) Guex, N.; Peitsch, M. C. *Electrophoresis* **1997**, *18*, 2714−23.
(49) Braden, B. C.; Velikovsky, C. A.; Cauerhff, A. A.; Polikarpov, I.; Goldbaum, F. A. *J. Mol. Biol.* **2000**, *297*, 1031−6.
(50) Royant, A.; Noirclerc-Savoye, M. *J. Struct. Biol.* **2011**, *174*, 385−90.
(51) Dormitzer, P. R.; Sun, Z. Y.; Wagner, G.; Harrison, S. C. *EMBO J.* **2002**, *21*, 885−97.